International Journal for Housing Science and Its Applications
Publish August 10, 2025. Volume 46, Issue 4 Pages 3597-3613

https://doi.org/10.70517/ijhsa464487a

Role of different proportions of steel slag based concrete on strength enhancement in highway pavement engineering

Liang Chen[1,*] and Qiang Shu[1]
[1] Chongqing University of Posts and Telecommunications, Chongqing, 400065, China
Corresponding authors: (e-mail: chenliang_cqupt@163.com).

Abstract This test proposes to use steel slag-based to replace part of the cement to prepare steel slag-based concrete for highway pavement construction, aiming at exploring the enhancement of the road performance of cement concrete and at the same time, providing a channel of resource utilization for steel slag waste. The shrinkage-cracking properties of steel-slag-based concrete were examined using the elliptical ring confinement method. The degree of influence of different mix ratios on the performance of the concrete specimens was derived from the abrasion resistance and physical strength of the concrete specimens through the tests, respectively. The experiments showed that: in the range of 0-40% admixture, with the increase of steel slag admixture, the slump of steel slag-based concrete becomes larger, and under the condition of standard curing at 28d age, when the admixture of steel slag micronized powder is more than 30%, the flexural tensile strength of steel slag-based concrete is more than 5.0MPa, which meets the requirements of the flexural tensile strength of concrete pavement of heavy-duty traffic loading grade.

Index Terms steel slag base, road performance, elliptical ring confinement, fit ratio, flexural tensile strength

I. Introduction

China's rapid economic growth, infrastructure construction has entered the fast lane. However, while China's infrastructure continues to improve, it is bound to consume a large amount of stone, which in turn leads to a scarcity of natural resources [1]. Under the premise of ensuring the current high speed of social and economic development and avoiding the deterioration of the ecological environment, how to realise the green low-carbon economy, promote the sustainable development of the economy, society and the environment, and find the alternative materials of natural aggregates are the key tasks that need to be dealt with urgently nowadays. Steel slag concrete has high strength and good abrasion resistance, and its application in road structure can effectively improve the ability of pavement to resist load deformation, prolong the service life of the road, save resources and also reduce the cost of late maintenance, with a wide range of development space and application prospects [2], [3].

Steel slag concrete material produces very high advantages and roles. First of all, its price is low, steel slag belongs to a waste, the cost is very low [4]. And has strong wear resistance, steel slag contains a single iron and other metal type elements, has an irregular shape, as an aggregate application can form a skeleton embedded extrusion type structure [5], [6]. In addition, steel slag concrete has strong adhesion properties, and the steel slag and bonding surface are not affected by water [7]. The steel slag without fine grinding has the characteristic of obvious microscopic pore structure, when contacting with asphalt, the asphalt gradually penetrates into the micropores of the steel slag, the contact area is increasingly expanding, becoming a structural asphalt, asphalt and steel slag bonding strength is subsequently enhanced, so the steel slag is used as an aggregate in asphalt concrete [8]-[11]. Steel slag concrete and ordinary concrete compared to see there is no big difference, take crushing, processing and dust removal in processing into steel slag raw materials, add asphalt and filler mixing, transported to the construction site, according to the mechanical paving and rolling can be shaped [12]-[15].

Due to its excellent properties, steel slag has been widely used as a raw material in road projects.Parron-Rubio María. et al. showed that the use of steel slag concrete as a construction material achieves the objectives of reducing raw material consumption and waste management at the same time, i.e., it reduces the high environmental damage caused by the production of cement, as well as treating and utilising by-products of the iron and steel industry production, which contributes to sustainable development [16]. Li, L. et al. found that the use of steel slag in pavement concrete paving brings great environmental performance, its use as a substitute for natural aggregates, on the one hand, avoids the use of large quantities of cement and reduces the consumption of environmental resources, on the other hand, the alkaline silicate minerals in steel slag act as a suitable material

for carbon capture, which is conducive to the slowing down of global warming [17].Zeynep, Y. I. et al. pointed out that steel slag has the shear strength and stiffness properties make it ideally suited as a material for both bonded and unbonded pavement layers, but its long-term dissolution, corrosion and leaching properties are of equal concern [18].Loureiro, C. D. A. et al. made it clear that the incorporation of wastes and by-products into asphalt mixtures for road surfaces has functional, mechanical and environmental advantages, but there is a need to focus on discussing and analysing the recycled concrete aggregate with respect to its possible disadvantages to achieve sustainable development of road paving projects [19].

The performance strength of steel slag concrete is the key to influence the utilisation of highway pavement projects, and a reasonable proportioning study of steel slag concrete to get its optimum admixture in mixed concrete is a prerequisite for steel slag to be used in practical projects. Mo, L. et al. investigated the potential use of accelerated carbonation of steel slag for the preparation of low carbon emission concrete by preparing a binder mix containing 60% steel slag powder possessing a high level of free CaO, 20% silicate cement, and 20% activated magnesium oxide and lime, and the compressive strength of this steel slag concrete was significantly increased after accelerated curing with CO_2 [20]. Kim, S. et al. used glycine as an activator to improve the mechanical properties of steel slag concrete under CO_2 curing conditions, and experiments showed that the microstructure of the cement binder in this ratio was significantly densified and the compressive strength was significantly increased after 1 day of hydration followed by 7 days of carbonation [21]. Li, Y. et al. compared the leaching properties, structure and toxicity of multi-solid waste composite pavement base materials (PBMs) based on steel slag (SS) and red mud (RM) with different Ca/(Si + Al) ratios, which provided a theoretical guideline for the application of solid waste in large quantities [22]. Liu, J. et al. tested the effect of different steel slag contents in steel slag concrete on the mechanical and durability properties of the mixes and the experimental and observational results showed that the mixes had the strongest combination of properties when the steel slag content was 50 per cent [23]. S., N. et al. explored the workability and strength properties of reactive powder concrete (RPC) under recycled concrete waste replacement and found that low water-cement ratio and steel fibres play an important role in strength development and durability properties of RPC and that the best strength properties exhibited by RPC were achieved at a content of 15% [24].

The innovation of this paper lies in the use of steel slag micropowder to replace part of the cement to prepare steel slag-based concrete, which is applied in highway pavement construction, aiming at exploring the enhancement of the performance of cement concrete pavement, but also to provide a channel for the resource utilization of steel slag waste, to provide a new choice for the concrete pavement material, to save the amount of cement and at the same time to enhance the economic, ecological and environmental benefits. Steel slag micropowder was used to prepare steel slag-based concrete by replacing part of the cement with 0%, 10%, 20% and 30% by mass fraction. The working properties, flexural strength and compressive strength of steel slag-based concrete were experimentally investigated by using different composite ratios of steel slag-cement composite cementitious materials. An elliptical ring constrained cracking automatic monitoring test device was used to test the shrinkage cracking properties of steel slag concrete cube specimens. The recommended optimum admixture of steel slag micronized powder was finally obtained.

II. Experimental materials and methods

II. A. Raw materials

The raw materials of steel slag-based concrete are roughly the same as those of ordinary concrete, mainly including cementitious materials, aggregates, water, admixtures and so on. The materials used in the experimental process of the content studied in this project are steel slag, fly ash, silica fume, cement, natural coarse and fine aggregates, steel slag sand, admixtures, and water. Steel slag-based concrete is intended to be designed as a green low-carbon concrete, and some of its performance tends to be high-performance concrete, which needs to meet the application of highway pavement projects to maintain good working performance, mechanical properties, durability and other related technical requirements, so it is necessary to meet the relevant specifications and standards when selecting materials.

II. A. 1) Cement

Cement is used as the main cementitious material in this study, and the composition of its chemical elements has a very important influence on all aspects of the final concrete properties, as well as the coordination with other cementitious materials. In this paper, P.O42.5 grade cement produced by local cement factory was used, and its basic performance indexes are shown in Table 1 and Table 2. The cements used satisfy the relevant performance requirements of GB175-2007 “General Silicate Cement”.

Table 1: Performance indexes of Portland cement

Item		Measured value	Standard limit
Apparent density (g/cm3)		3.05	-
Setting time	Initial coagulation (min)	134	≤45
	Final coagulation (min)	205	≤400
Intensity	3d Compressive resistance (MPa)	20.25	≥16.5
	28d Compressive resistance (MPa)	48.32	≥42.5
	3d Flexural strength (MPa)	4.56	≥3.0
	28d Flexural strength (MPa)	7.81	≥6.0

Table 2: Chemical composition and content of cement

Chemical composition	Content %
SiO_2	21.84
Al_2O_3	4.52
CaO	64.15
MgO	1.93
Na_2O	0.45
K_2O	0.75
TFe_2O_3	5.11
SO_3	0.89
TiO_2	0.15
MnO	0.11
P_2O_5	0.08
V_2O_3	0.02

II. A. 2) Steel slag base

Steel slag base is a steel slag base by-product composed of the corresponding oxides formed by the oxidation of sulfur, silicon, phosphorus, manganese and other impurities in pig iron in the steelmaking process and the compounds generated by the reaction between the flux and these oxides. Its main components and content are shown in Table 3.

Table 3: Steel slag chemical composition and content

Chemical composition	MgO	f-CaO	SiO_2	Fe_2O_3	MnO	Al_2O_3	CaO	RO_2
Content %	9.22	0.89	29.35	4.27	1.12	8.15	45.12	1.88

(1) Steel slag powder

Steel slag can be used in concrete as a cementitious material instead of cement due to the similarity between its composition and that of silicate cement. However, due to its generation environment temperature is higher than the temperature of silicate cement clinker generation environment of more than 100 ℃, resulting in the steel slag will have some impurities into the crystallization, which in turn limits the development of its activity. Utilizing grinding technology, steel slag can be finely ground to the degree of micronized powder, which can improve the activity of steel slag when it interacts with the aqueous phase.

The steel slag powder used in this test, selected from the local mineral processing plant, has a particle size of less than 200 mesh, and its main technical indicators are shown in Table 4.

Table 4: Main technical indexes of steel slag powder

Specific surface area (m2/kg)	Fluidity (%)	Water content (%)	Stability	Activity index (%)	
				7d	28d
360	125	0.67	Up to standard	67	82

(2) Steel slag sand

The application of steel slag as aggregate in concrete can reduce the use of natural sand and gravel while solving the problem of large amount of steel slag accumulation, in addition to improving the performance of concrete to a certain extent. The two grain sizes of steel slag sand used in this study, and their main technical specifications are shown in Table 5. One is the steel slag sand from local mineral processing plant, which has a more regular grain shape and a grain size of 5 mesh to 20 mesh. One is a larger particle size of steel slag stone, its particle size is more than 110mm, the use of school tools will be crushed to obtain the particle size of 4.5mm or less steel slag sand, steel slag sand particles are mostly sharp corners, flaky predominant.

Table 5: Main technical indexes of steel slag sand

Category	Packing density (kg/m3)	Apparent density (kg/m3)	Water absorption (%)
Steel slag sand (≤ 4.5mm)	1448	2956	3.82
Steel slag sand (5 ~20 mesh)	1593	3227	3.68

II. A. 3) Aggregates and admixtures

(1) Silica fume

Silica fume, also known as microsilica powder, is collected from the soot emitted in the smelting process of metals related to silicon, mostly in gray or off-white color, the lighter the color indicates that the quality of microsilica powder is better. Its main component is silicon dioxide, the content of more than 80%, the higher grade of micro-silica powder in the silicon dioxide content of even more than 90%. The use of microsilica powder as concrete admixture can significantly improve the strength of concrete, and when used together with steel slag powder can also improve the durability and workability of concrete. To a certain extent, it improves the quality and durability of concrete.

The microsilica powder selected in this test comes from Jinhua Mining Co. and meets the performance requirements for microsilica powder in GB/T18736-2017 “Mineral Admixtures for High Strength and High Performance Concrete” and other specifications.

(2) Fly ash

Fly ash is the fly ash collected from the flue gas of coal combustion and has high volcanic ash activity. The application of high quality fly ash as cementitious material in concrete is helpful in workability and durability. Compound mixing of fly ash and steel slag micronized powder can significantly improve the late strength of concrete, and also have some improvement on the durability performance of concrete.

The fly ash used in this test was provided by the fly ash company, and its basic performance requirements meet the specifications such as GB/T18736-2017 Mineral Admixtures for High Strength and High Performance Concrete.

(3) Water reducing agent

Appropriate mixing of admixtures in concrete, clever use of workability and water-cement ratio, water consumption is low in the case of the contradiction between, can improve the early mechanical properties of concrete, and at the same time increase the cohesion between the components in the concrete, water retention of concrete, reduce the loss of time and so on. Water reducing agent as an important component of concrete, although its dosage is very small, but it can improve many properties of concrete.

The fly ash used in this test is provided by the fly ash company, and its basic performance requirements meet the specifications such as GB/T18736-2017 Mineral Admixtures for High Strength and High Performance Concrete.

II. B.Experimental Methods

II. B. 1) Mechanical performance test

(1) Compressive strength test

This test uses the side length of 100 × 100 × 100mm non-standard cubic specimens, the measured strength values are multiplied by the size of the conversion factor of 0.95, the test using a microcomputer-controlled automatic 300T pressure testing machine.

Steel slag-based concrete cubic specimen compressive strength calculation formula:

$$f_{cc} = \frac{F}{A} \tag{1}$$

where, f_{cc} - Compressive strength of concrete cube specimen (MPa), F - specimen destructive load (N), A - specimen pressure-bearing area (mm^2).

(2) Splitting tensile strength test

The side length of 100 × 100 × 100mm non-standard cubic specimens, the measured strength values are multiplied by the size conversion factor of 0.85, the test using a microcomputer-controlled automatic 300T pressure testing machine.

Steel slag-based concrete splitting tensile strength calculation formula:

$$f_{ts} = \frac{2F}{\pi A} = 0.637\frac{F}{A} \tag{2}$$

where, f_{ts} - concrete splitting tensile strength (MPa), F - specimen breaking load (N), A - specimen cracking surface area (mm^2).

(3) Axial compressive strength test

This test uses a non-standard prismatic specimen with a side length of 100 × 100 × 300 mm, the measured strength values are multiplied by the size conversion factor of 0.95, and the test is conducted using a microcomputer-controlled automatic 300T pressure testing machine. During the test, the test was continuously and uniformly loaded at a speed of 0.5 MPa/s.

The compressive strength of steel slag concrete cube specimens was calculated as:

$$f_{cp} = \frac{F}{A} \tag{3}$$

where, f_{cp} - Axial compressive strength of concrete (MPa), F - specimen breaking load (N), A - Specimen pressure-bearing area (mm^2).

(4) Static compression modulus of elasticity test

During the test, the upper loading plate is contacted with the test piece, and the ball hinge is adjusted to equalize the contact. Load at 0.25MPa/s to the initial load F_0 (about 0.8MPa), hold for 80s, then load at 0.5MPa/s continuously and uniformly to F_a (axial compressive strength of 1/3 of the load value of f_{cp}), hold for 80s, to determine the front and back of the two specimens on both sides of the deformation of the difference between the deformation of more than the average value of deformation of 20%, otherwise re-location of specimen position.

Repeat the above steps to complete the two preloading, the last loading to the initial load F_0, hold for 80s, read the average value of the deformation of both sides of the micrometer calculated ε_0, then load to F_a, hold for 80s, read the average value of the deformation of both sides of the micrometer calculated ε_a, and find the average value of the deformation of both sides of the test specimen when the last loading from F_0 to F_a, Δn. Then, unloading the micrometer, and continue to load the specimen at the same speed. Then remove the micrometer and continue loading at the same rate until the specimen is damaged, and record the cyclic axial compressive strength. The value of modulus of elasticity of concrete in static compression is calculated as:

$$E_c = \frac{F_a - F_0}{A} \times \frac{L}{\Delta n} \tag{4}$$

$$\Delta n = \varepsilon_a - \varepsilon_0 \tag{5}$$

where, E_c - Modulus of elasticity of concrete under hydrostatic stress (MPa), F_a - the load (N) when the stress is the axial compressive strength, F_0 - Initial load (N) at a stress of 0.5 MPa, A - Specimen pressure-bearing area (mm^2), Δn - Average value of deformation on both sides of the specimen at the last loading from F_0 to F_a (mm), ε_a - average value of deformation on both sides of the specimen at F_a (mm), ε_0 - Average value of deformation on both sides of the specimen at F_0 (mm).

II. B. 2) Shrinkage cracking limitation tests

In this paper, an elliptical ring constrained cracking automatic monitoring test setup as shown in Fig. 1 is used to test the shrinkage cracking properties of steel slag concrete cube specimens. The test setup includes the sample ring to be tested, the restraining mold, the conductive body, the signal generator and the data collector. The main working principle is that the core elliptical restraining mold forms a restraining effect on the elliptical ring specimen to be tested, and the specimen is more likely to crack due to stress concentration. Automatically collect the data of

resistance in the loop over time, when the concrete tensile stress exceeds its tensile strength to form a crack, cracking instant resistance in the loop appears sudden change, automatically record the crack time, and based on the crack time to judge the specimen under the constraint conditions of the sensitivity of cracking.

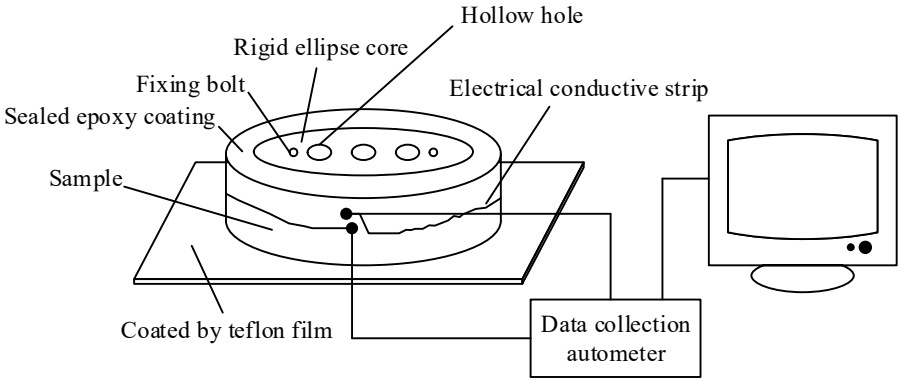

Figure 1: Automatic monitoring test device for elliptical ring constraint cracking

The dimensions of the elliptical ring specimens of steel slag concrete in this study are shown in Fig. 2. The length of the elliptical ring half-length axis is 105 mm and the half-short axis is 45 mm. The half-length axis of the outer elliptical ring is 125 mm and the half-short axis is 65 mm. In order to form the constraints at the same time to reduce the weight of the equipment with the maximum efficiency, the elliptical ring and the height of the molds are both 50 mm.

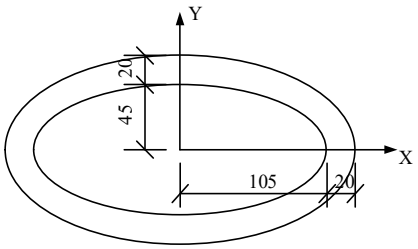

Figure 2: Elliptical ring specimen size

Figure 3 shows the variation of the thickness of the elliptical ring specimen, which is defined as the minimum distance from the point at the inner circumference (point B) to the point at the outer circumference (point A), then:

$$|AB|^2 = \left[(a+t)\cos\theta_1 - a\cos\theta\right]^2 + \left[(b+t)\sin\theta_1 - b\sin\theta\right]^2 \quad (6)$$

where a and b are the semi-long and short major axes of the inner ellipse, respectively; t is the deviation of the semi-major axis between the inner and outer ellipse, and θ_1 and θ are the polar angles of the points A and B when expressed in polar coordinates. Taking the differentiation of the equation with respect to θ and using Newton's interpolation, a numerical solution for the ring thickness at the point can be obtained.

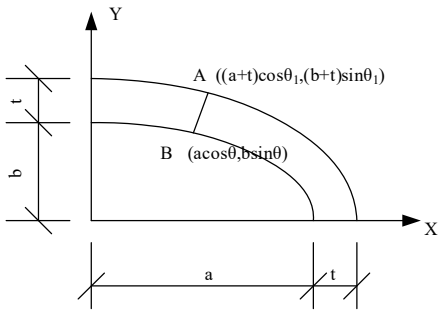

Figure 3: Variation in thickness of elliptical ring specimens

Assuming that the center elliptical steel block provides uniform pressure to the specimen, the annular and radial stress variations along the elliptical ring specimen are shown in Fig. 4. The stress variation at the free position is shown in Fig. 4(a). The pressure applied to the elliptical ring specimen piece from $A_1(x_1, y_1)$ to $A_2(x_2, y_2)$ along the X direction is:

$$F_x = \int_{\alpha}^{\alpha_2} pdA\cos\phi = \int_{n_1}^{y_2} p\frac{dy}{\cos\phi}\cos\phi = \int_{n_1}^{y_2} pdy = p(y_2 - y_1) \tag{7}$$

The pressures $A_1(x_1, y_1)$ to $A_2(x_2, y_2)$ applied to the elliptical ring specimen piece are:

$$F_x = \int_{\alpha}^{\alpha_2} pdA\cos\phi = \int_{n_1}^{y_2} p\frac{dy}{\cos\phi}\cos\phi = \int_{n_1}^{y_2} pdy = p(y_2 - y_1) \tag{8}$$

Similarly, the pressure applied to the same portion of the elliptical ring specimen along the Y direction is:

$$\begin{aligned} F_y &= \int_{\alpha}^{Q_2} pdA\sin\phi = \int_{x_1}^{x_2} p\frac{-dx}{\sin\phi}\sin\phi \\ &= \int_{x_1}^{x_2} -pdx = \int_{x_2}^{x_1} pdx = p(x_1 - x_2) \end{aligned} \tag{9}$$

where the variables σ_{r0} and $\sigma_{\theta 0}$ are defined as the radial and circumferential stresses at $x = a$ and $y = 0$, respectively. It can be seen that according to the symmetry of the X-axis, the radial stress σ_{r0} is zero, while the circumferential stress $\sigma_{\theta 0}$ can be determined as according to Eq:

$$F_y = 2\sigma_{\theta 0}t = \int_{a}^{-a} pdx = p(a - (-a)) = 2pa \tag{10}$$

Then:

$$\sigma_{\theta 0} = \frac{2pa}{2t} = \frac{pa}{t} \tag{11}$$

If the free position of the elliptic ring is considered in the range $S(a,0)$ to $A(X_a, Y_a)$ in the Cartesian coordinate system is shown in Fig. 4(b).

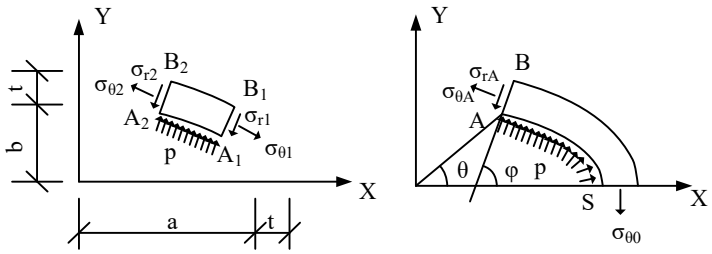

(a) Free position

(b) Position change from x=1, y=0

Figure 4: Circumferential and radial stress variations along elliptical ring specimens

and assuming that the normal at point $A(X_a, Y_a)$ has a slope of ϕ, the circumferential stresses $\sigma_{\theta A}$ and σ_{rA} radial stresses acting on the cross-section can be obtained from the equilibrium forces along the directions X and Y, respectively, as follows:

$$-\sigma_{\theta A}t_A\sin\phi - \sigma_{rA}t_A\cos\phi + \int_0^{r_A} pdy = 0 \tag{12}$$

$$\sigma_{\theta A}t_A\cos\phi - \sigma_{rA}t_A\sin\phi + \int_{X_A}^{a} pdx - pa = 0 \tag{13}$$

Solving the equation yields:

$$\sigma_{\theta A}t_A = pX_A\cos\phi + pY_A\sin\phi \tag{14}$$

$$\sigma_{rA}t_A = -pX_A\sin\phi + pY_A\cos\phi \tag{15}$$

Bring it in:

$$\sin\phi = \frac{a^2Y_A}{\sqrt{(a^2Y_A)^2 + (b^2X_A)^2}} \tag{16}$$

$$\cos\phi = \frac{b^2 X_A}{\sqrt{\left(a^2 Y_A\right)^2 + \left(b^2 X_A\right)^2}} \tag{17}$$

The equations for the annular and radial stresses in the concrete elliptic ring are obtained:

$$\sigma_{\theta A} t_A = \frac{p\left(a^2 Y_A^2 + b^2 X_A^2\right)}{\sqrt{\left(a^2 Y_A\right)^2 + \left(b^2 X_A\right)^2}} \tag{18}$$

$$\sigma_{rA} t_A = \frac{p\left(-a^2 + b^2\right) X_A X_A}{\sqrt{\left(a^2 Y_A\right)^2 + \left(b^2 X_A\right)^2}} \tag{19}$$

During the test monitoring, set the strain value of the inner surface of the steel ring in the elliptic ring to be automatically collected every 5 min, with the strain gauge resistance value (120.5±0.2) Ω and the sensitivity coefficient (2.05±0.5)%. Observe and record the elliptical ring strain over time graph, when the strain curve shows an increase or decrease of hundreds of micro-strain, that is, the early concrete cracking time.

II. B. 3) Abrasion tests

The experiment was operated in accordance with JGE30-2005 Experimental Procedures for Cement and Cement Concrete in Highway Engineering, and the size of the wear-resistant specimen was 100mm×100mm×100mm cubic specimen. Firstly, the specimens of 3d and 28d maintenance age were taken out to dry the excess water on the surface, placed in the air to dry naturally for 12h, and then put into the constant temperature drying box at 55±5℃ to dry for 12h to constant weight. Then, the mass of the test piece was M1 after grinding 10 revolutions under the load of 300N and cleaning the surface dust, and finally, the mass of the test piece was M2 after grinding 50 revolutions under the load of 300N and cleaning the surface dust, and the wear amount per unit area, G_c, was calculated by the formula:

$$G_c = \frac{M_1 - M_2}{0.0175} \tag{20}$$

where, G_c - wear per unit area $\left(kg/m^2\right)$, M_1 - Initial mass of the specimen $\left(kg\right)$, M_2 - mass of the specimen after wear $\left(kg\right)$, 0.0175 - Surface area of the test piece worn $\left(m^3\right)$.

II. B. 4) Dry and wet cycle experiments

Depending on the use of cement concrete in engineering, its immersion environment under rainwater is not the same. In this paper, the steel slag-based concrete is designed to be used in highway pavement, and the concrete is under intermittent water immersion.

In this paper, the dry and wet cycle experiments using simulated intermittent immersion method, to study the different steel slag-based concrete substitution amount of cement concrete specimens in the dry and wet role of the strength of the change rule, and to evaluate its advantages and disadvantages. The specific method of intermittent immersion:

(1) Put the specimen with good concrete curing into tap water and soak it for the corresponding time.

(2) Take them out to dry naturally, and then put them into the oven at the appropriate temperature to dry.

(3) Soak them in water again.

The above process is a cycle, and so on repeatedly cyclic operation for a number of cycles to carry out this test.

II. C.Test piece preparation

Concrete is a multi-phase mixture of cement, coarse aggregates, fine aggregates, water and chemical admixtures, etc., which is mixed and hardened after curing. The design of concrete proportion is mainly through the calculation, adaptation, debugging method to determine the amount of each material in the concrete, so that the poured concrete in both its performance and at the same time to meet the economy, saving the amount of materials and reduce costs, in response to the government's proposal of the resourcefulness and efficiency.

The macroscopic performance indexes and internal microstructure of steel slag-based concrete and ordinary concrete are largely the same, and there are only some minor differences. When preparing ordinary concrete, it is mainly designed with strength indexes, while also taking into account ease and durability, etc. Reasonable cement concrete ratio is the key factor to realize the concrete casting and determine its physical properties.

Cement concrete with different mixing ratios can have differences in its internal structure, because the internal structure of concrete often determines its macroscopic properties, so differences in mixing ratios can lead to

differences in concrete properties. Designing a reasonable mix ratio is a key factor in realizing the function of concrete. According to the research purpose of this paper and the relevant specifications to design the mix ratio, the design specifications mainly refer to the “Modern Concrete Mix Ratio Design Manual”, as well as the “Highway Cement Concrete Pavement Design Specification”.

II. C. 1) Steel slag base dosing

Existing research on the single mix of steel slag base to replace part of the cement to prepare cement concrete is relatively small, most of them are compounded into other materials, some scholars have conducted research on the use of steel slag base as a modified material modified with lower quality fly ash to prepare fly ash concrete [25]. Experiments have proved the feasibility of steel slag-based cement concrete, and more short-term road performance experiments were conducted on it, and the comprehensive indexes recommended that the amount of steel slag-based replacement of cement is more appropriate between 20% and 25% [26].

In this paper, firstly, the amount of steel slag base replacing cement is selected as 0%, 10%, 20% and 30% to design the C30 steel slag base concrete proportion. Then the specimens are prepared according to the mix ratio, and finally the road properties of the concrete are compared and analyzed.

II. C. 2) Mixing ratio design

According to the “Design Code for Highway Cement Concrete Pavement” (JTG40-2011), the specification stipulates that the bending and tensile strength of different grades of road is shown in Table 6. In the case of standard curing 28d, the specimen bending and tensile strength is not less than 5MPa, slump is less than 100 mm is appropriate, apparent density is more than 2400 $\mathrm{kg/m^3}$.

Table 6: Flexural tensile strength of different grades of roads

Load grade	Very heavy, extra heavy, heavy	Medium	Light
Flexural tensile strength	≥5 MPa	≥4.5 MPa	≥4.0 MPa
Collapse depth	≤100 mm	≤120 mm	≤200 mm
Apparent density	≥2400 $\mathrm{kg/m^3}$	≥2100 $\mathrm{kg/m^3}$	≥1600 $\mathrm{kg/m^3}$

According to the specification of “Highway Cement Concrete Pavement Construction Technical Rules” (JTG/T F30-2014), the steel slag-based concrete proportion design is carried out, and the specific steps are as follows:

(1) Determination of 28d flexural strength of concrete:

$$f_c = \frac{f_r}{(1-1.04C_v)} + ts = 5.50 \tag{21}$$

where, f_c - Test concrete formulated strength, f_r - Design concrete strength standard, 5 MPa, s - standard deviation of the bending and tensile strength test samples, the standard deviation s value of the samples of the reference road concrete is shown in Table 7, and the s is taken to be 0.3 for the application of concrete to highways in this study, C_v - bending and tensile strength coefficient of variation, pavement concrete bending and tensile strength coefficient of variation is shown in Table 8, the value of this test is taken as $C_v = 0.05$, t - Assurance rate coefficient, which takes the value shown in Table 9, and is taken as $t = 0.060$ for this test.

Table 7: Sample standard deviation s value

Highway grade	Highway	First-order	Second level	Three level	Four level
Target reliability	95%	90%	85%	80%	70%
Target reliable indicators	1.65	1.31	1.05	0.85	0.60
Standard deviation of sample s (MPa)	0.25≤s≤0.5	0.40≤s≤0.65		0.40≤s≤0.80	

Table 8: Variation coefficient of flexural tensile strength of pavement concrete

Highway grade	Highway	First-order	Second level	Three and four level	
Coefficient of variation Cv of flexural tensile strength	Low	Low	Medium	Medium	High
	0.02-0.10	0.02-0.10	0.10-0.20	0.10-0.20	0.20-0.30

Table 9: Value of the retention ratio coefficient t

Highway grade	Discriminant probability P	Sample size n (group)			
		6-9	10-15	16-20	≥21
Highway	0.05	0.81	0.62	0.43	0.41
First-order	0.10	0.60	0.47	0.29	0.32
Second level	0.15	0.45	0.38	0.28	0.25
Three and four level	0.20	0.36	0.27	0.25	0.22

(2) Determination of water-cement ratio:

$$W/C = \frac{1.5685}{\left(f_c + 1.0097 - 0.3595 f_s\right)} = 0.454 \tag{22}$$

where, f_s - cementitious sand 28d age flexural tensile strength, is 8.5MPa, f_c - Test concrete formulated strength.

(3) Determination of sand content rate

According to the “Highway Cement Concrete Pavement Construction Technical Rules” (JTG/T F30-2014) specification of the relationship between the fineness modulus of sand and the optimal sand rate is shown in Table 10, and the sand rate used in this study is 34%.

Table 10: The relationship between the fineness modulus of sand and the optimal sand rate

Sand fineness modulus	2.0-2.5	2.5-2.8	2.8-3.2	3.2-3.5	3.4-3.8
Optimal sediment rate Sp	30-35%	32-38%	34-40%	36-42%	38-44%

(4) Water consumption per unit

$$W_0 = 107.08 + 0.309 S_L + 11.27\, C/W + 0.61 S_P = 183.35 Kg \tag{23}$$

Actual water consumption after adding polycarboxylic acid water reducing agent:

$$W_1 = W_0\left(1 - \beta\right) = 137.51 Kg \tag{24}$$

where, S_L - set slump of concrete, 100mm, S_P - Preliminary match ratio sand rate, 34%, β - Polycarboxylic acid water reduction, 25%.

(5) Unit amount of cementitious material:

$$B_0 = 183.35/0.45 = 407.44\mathrm{Kg} \tag{25}$$

(6) Actual water-cement ratio:

$$W/B = W_1/B_0 = 137.51/407.44 = 0.3375 \tag{26}$$

The durability requirements of cement concrete for highway surfaces at all levels, and the conditions to be met by the water-cement ratio are shown in Table 11.

Table 11: Maximum water-cement (glue) ratio

Highway grade	Highway, First-order	Second level	Three and four level
Maximum water ash (glue) ratio	0.45	0.47	0.49
Maximum water-cement (glue) ratio when frost resistance is required	0.40	0.43	0.46
Maximum water-cement (glue) ratio when salt-freeze resistance is required	0.40	0.42	0.44
Minimum unit cement usage kg/m3 ((Level 42.5))	320	310	300

(7) Unit fine aggregate usage:

$$\left(2400 - B_o - W_1\right) \times S_P = \left(2400 - 407.44 - 137.51\right) \times 34\% = 630.717\mathrm{Kg} \tag{27}$$

(8) Unit crude aggregate usage:

$$\left(2400 - B_o - W_1\right) \times \left(1 - S_P\right) = \left(2400 - 407.44 - 137.51\right) \times 66\% = 1224.333\mathrm{Kg} \tag{28}$$

(9) Finally, the steel slag based concrete mixes for highway were obtained as shown in Table 12. In this paper, four types of specimens (C0~C30) were designed based on 0%, 10%, 20% and 30% of the amount of cement replaced by steel slag base.

Table 12: Mix ratio of steel slag base concrete for highway traffic

Ingredients		Steel slag replacement rate (%)			
		C0	C10	C20	C30
		0%	10%	20%	30%
Cement		381	372	365	352
water		140.52	153.42	167.16	171.62
Water-binder ratio		0.40	0.40	0.40	0.40
Sand Ratio		35%	35%	35%	35%
Water reducing agent		3.85	3.74	3.61	3.56
Fine aggregate		635.67	652.34	660.08	667.20
Coarse aggregate /mm	15-25	372.58	341.25	356.52	354.25
	9.2-15	493.57	483.11	473.90	465.44
	4.5-9.2	395.56	381.25	372.45	367.21

III. Experimental study of the properties of steel slag-based concrete

III. A. Analysis of physical properties of steel slag based concrete

III. A. 1) Effect of different mix ratios on compressive strength of concrete

The compressive strength development trend of steel slag based concrete with the increase of steel slag fine aggregate admixture is shown in Fig. 5. The increase in the substitution rate of steel slag fine aggregate resulted in a significant increase in the compressive strength of the specimens at all ages, especially at the later stages. Compared with the concrete without steel slag fine aggregate (C0), the 28d compressive strengths of C10, C20, and C30 specimens were 42.022 MPa, 48.5039 MPa, and 51.1717, which were increased by 3.53%, 19.50%, and 26.07%, respectively. Under the condition of the same water-to-cement ratio, it is mainly related to the grading of steel slag fine aggregate, which is better than that of sea sand, and thus can effectively reduce the void ratio of concrete.

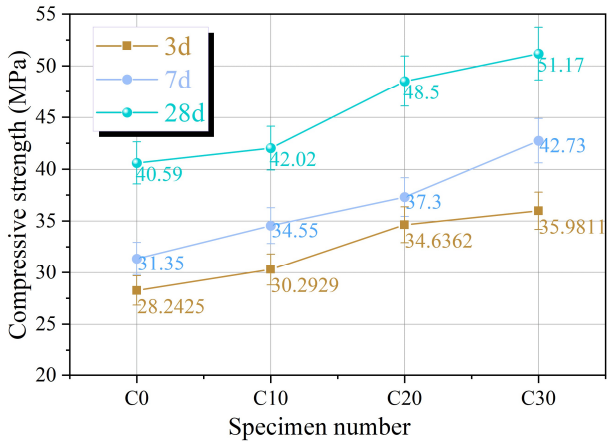

Figure 5: Influence of different blending ratio on compressive strength of steel slag concrete

The compressive strength of steel slag concrete is not only related to the binder and fine aggregate in it, but the coarse aggregate also plays a key role. Figure 6 shows the compressive strength of steel slag aggregate road concrete (labeled as HFPC), where HFPC-A~E refers to the change of the amount of steel slag coarse aggregate replaced by fine aggregate from 20%, 40%, 60%, 80, 100%. It can be seen that the compressive strength of the specimens with the increase in the amount of steel slag fine and coarse aggregate replacement and gradually improve, and the enhancement effect is obvious. 28d compressive strength of the specimens of HFPC-A (replacement of 20%) and HFPC-B (replacement of 40%) can reach the requirements of the C20 road concrete (30MPa), respectively, 30.01MPa and 35.15MPa. The compressive strength of another three groups of all-steel slag aggregate specimens can reach the C20 road concrete requirement (30MPa), respectively. The compressive strength of the other three sets of full steel slag aggregate specimens can reach the requirement of C30 concrete strength (50MPa), which is 85%~90% higher than that of HFPC-A specimens.

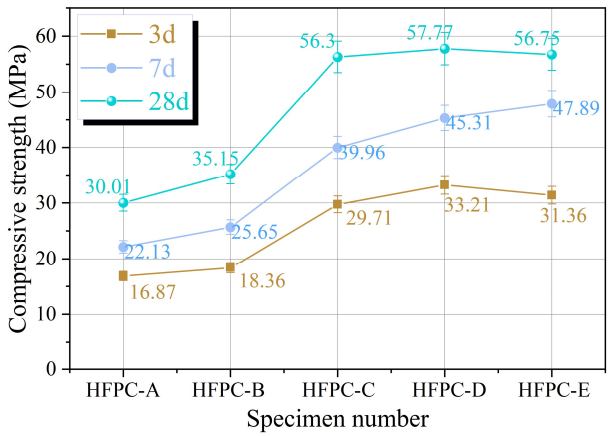

Figure 6: Compressive strength of steel slag aggregate pavement concrete

The improvement of strength by steel slag aggregate is not only related to its gradation optimization, but also closely related to its own characteristics and hydration reaction. In the late reaction stage, the compressive strength of the specimen is mainly determined by the strength of the binder, the strength of the aggregate and the bonding properties between their interfaces. Compared with natural aggregates, steel slag has higher hardness and rougher surface. Therefore, with the incorporation of steel slag aggregate, the compressive strength of the specimen is increased. From the hydration reaction point of view, there are some glass phases in the steel slag aggregate, which can participate in the secondary hydration reaction, improve the bond strength between the slurry and the aggregate, and enhance the compressive strength of the specimen.

III. A. 2) Effect of different mix ratios on flexural strength of concrete

(1) Steel slag fine aggregate

Flexural strength is one of the important parameters for evaluating the mechanical properties of road concrete materials, Figure 7 shows the effect of steel slag fine aggregate on the flexural strength of concrete. It can be seen that with the increase of steel slag fine aggregate dosage, the flexural strength of the specimens continued to increase. 3d, 7d, 28d flexural strength of C30 specimens were 6.83 MPa, 8.21 MPa, 8.69 MPa. Compared with the specimen C0 without steel slag fine aggregate, it was increased by 21.31%, 21.63%, and 19.20%, respectively.

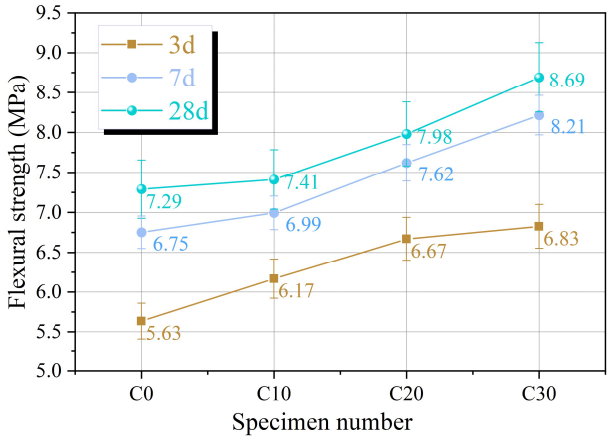

Figure 7: Influence of steel slag fine aggregate on flexural strength of concrete

(2) Steel slag coarse aggregate

When road concrete is designed for proportioning, its 28d flexural strength is often taken as the design index.CJJ37-2012 points out that the flexural tensile strength of cement concrete of the surface layer in road construction shall not be lower than 4.5MPa, and the flexural tensile strength of high speed road and heavy traffic road shall not be lower than 5.0MPa.

The flexural strength of HFPC is shown in Fig. 8, and it can be seen that the 3d, 7d and 28d flexural strengths of HFPC-A specimen are 3.29MPa, 3.92MPa and 4.61MPa respectively, which indicates that the actual flexural

strength of the specimen has reached the design requirements of ordinary road construction to the mix ratio (4.5MPa) With the increase of steel slag coarse aggregate doping, the flexural strength of the specimens continued to improve, and when the coarse aggregate reached more than 30%, i.e., HFPC-C, HFPC-D, HFPC-E specimens reached more than 5.0 MPa flexural strength at 28d, which is in line with the requirement of flexural tensile strength for high speed road and heavy traffic road (5.0 MPa). This may be caused by the rough surface of the steel slag coarse aggregate particles. With the incorporation of steel slag coarse aggregate, the inter-particle friction effect in the specimens is enhanced, and this effect is especially obvious in the early stage. The flexural strength results show that HFPC can be used not only in face cement concrete but also in important transportation roads.

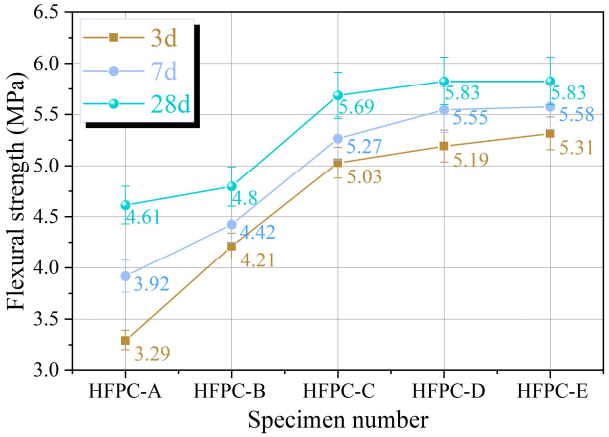

Figure 8: The flexural strength of HFPC

III. A. 3) Effect of different mix ratios on split tensile strength of concrete

(1) Steel slag fine aggregate

Splitting tensile strength is widely used in the performance evaluation of pavement materials as a reflection of the strength of plastic materials under the maximum pressure they can resist from deformation to cracking.

Figure 9 shows the effect of steel slag fine aggregate on the split tensile strength of concrete, and its trend is similar to that of compressive and flexural strength. In system C, the 3d, 7d and 28d splitting tensile strengths of the specimens, with the increasing dosage of steel slag fine aggregate, increased from 1.95MPa, 2.31MPa and 2.94MPa to 2.73MPa, 2.81MPa and 4.04MPa, respectively, which indicated that the steel slag fine aggregate has a positive effect on the development of concrete splitting tensile strength.

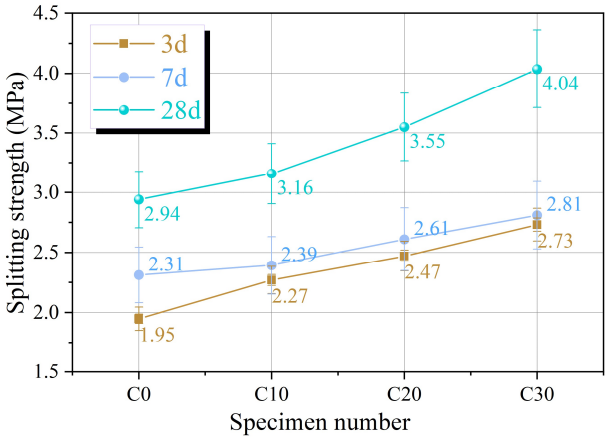

Figure 9: Influence of steel slag fine aggregate on the splitting tensile strength of concrete

(2) Steel slag coarse aggregate

Road concrete in the continuous vehicle load, crack resistance is particularly important, split tensile strength is another important parameter that can indirectly reflect the strength of concrete crack resistance.

The effect of steel slag coarse aggregate on the splitting tensile strength of road concrete is shown in Fig. 10, which shows that the splitting tensile strength of HFPC-C, HFPC-D and HFPC-E specimens in 3d and 28d are higher than that of HFPC-A and HFPC-B specimens. Their 28d splitting tensile strengths were 5.56 MPa, 5.66 MPa and 5.65 MPa, respectively, indicating that the large dosage of steel slag coarse aggregate was beneficial to enhance the splitting resistance of road steel slag-based concrete, and strengthened the tensile strain capacity under the action of long-term vehicular loading.

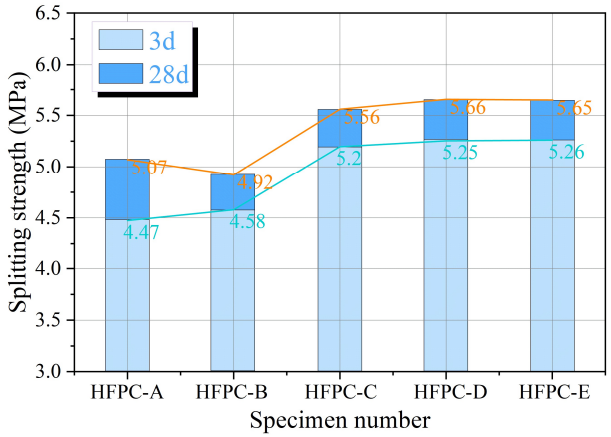

Figure 10: The splitting strength of HFPC

III. B. Analysis of steel slag-based concrete to limit shrinkage cracking

The automatic monitoring test device for elliptical ring restrained cracking was used to test the performance of steel slag-based concrete in restraining shrinkage cracking. The real-time strain of the steel ring was plotted as a function of time according to the real-time strain of the steel ring monitored by the IMC data acquisition system during the test.The strain curves of the steel ring of the three concrete restrained circular and elliptical ring specimens of C10, C20, and C30 are shown in Fig. 11. Among them, (a), (c) and (e) are the restrained circular ring specimens of the three kinds of concrete C10, C20 and C30, and (b), (d) and (f) are the restrained elliptical ring specimens of the three kinds of concrete. From the strain curves, it can be seen that at the beginning of concrete shrinkage, the steel ring produces compressive strain and the compressive strain increases rapidly. With the growth of age, the tendency of concrete shrinkage tends to level off, and the compressive strain of the steel ring gradually tends to stabilize. When the crack appears, the steel ring stress is released, and a clear hysteresis appears in the steel ring compressive strain curve. Based on the strain hysteresis in the steel ring compressive strain curve, the moment of crack appearance in the concrete ring specimen can be determined.

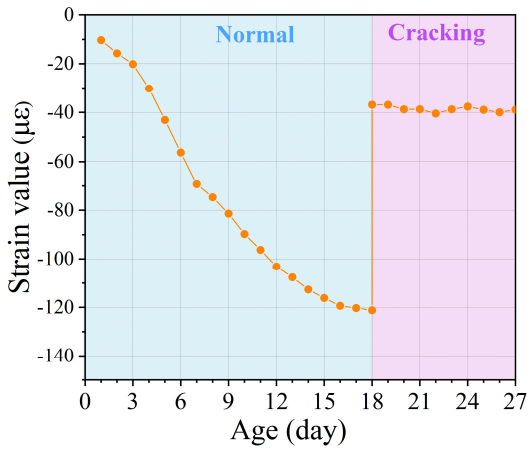

(a) C10-Ring specimen

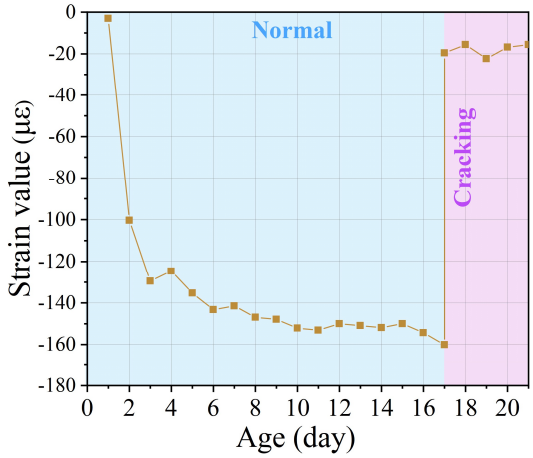

(b) C10-Elliptical ring specimen

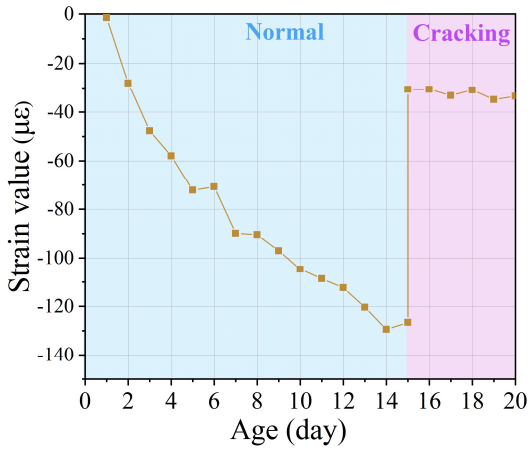

(c) C20-Ring specimen

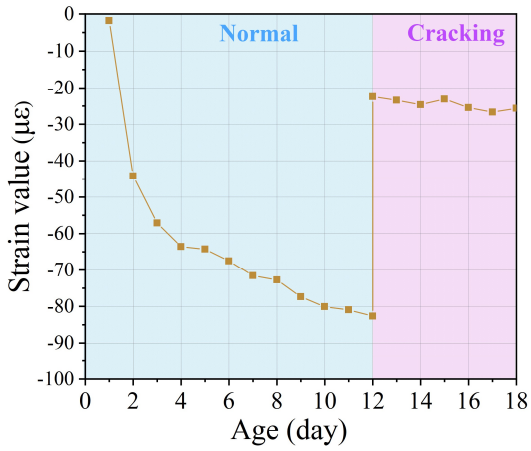

(d) C30-Elliptical ring specimen

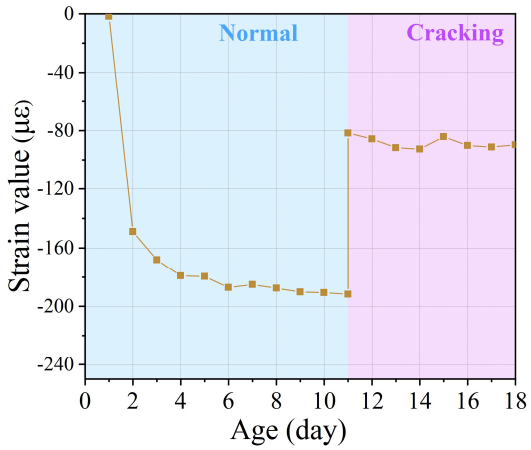

(e) C20-Ring specimen

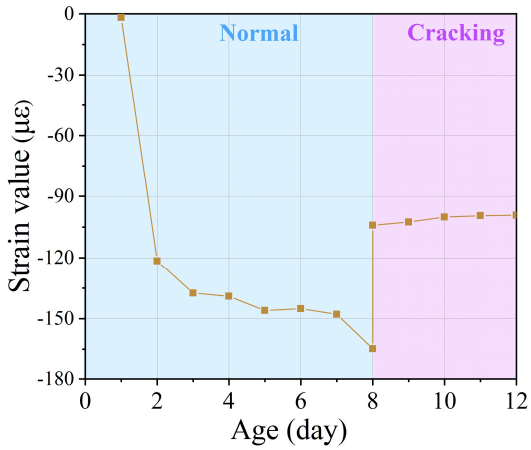

(f) C30-Elliptical ring specimen

Figure 11: Strain curves measured at the inner surface of steel rings

The average cracking times of the C10, C20, and C30 steel slag-based concrete restrained circular and elliptical ring specimens studied in this paper are shown in Table 13. It can be seen that the cracking times of the three typical high-strength steel slag-based concretes studied in this paper (C10, C20, and C30) have large differences, but show a certain pattern. the longest cracking time is observed for C10 steel slag-based concrete, followed by C20 steel slag-based concrete, and the shortest cracking time is observed for C30 steel slag-based concrete. This indicates that as the steel slag base admixture increases, the later the cracking time under the same constraints, i.e., the worse the cracking resistance. Although C30 steel slag based concrete has high compressive strength, flexural strength and splitting tensile strength, due to its high modulus of elasticity and shrinkage, C30 steel slag based concrete is more susceptible to cracking compared to other specimens.

Table 13: Average cracking age of the restrained ring test obtained by experiment

Concrete	C10	C20	C30
Confined ring specimen	18 Day	15 Day	11 Day
Constrained elliptic ring specimen	17 Day	12 Day	8 Day

IV. Conclusion

This paper draws the following conclusions through the study of the performance of steel slag cement composite cementitious material and the road performance, mechanical properties and limitation of shrinkage cracking performance of steel slag-based concrete with different mixing ratios:

(1) With the increase of steel slag coarse aggregate mixing, the flexural strength of steel slag-based concrete continues to improve, and when the coarse aggregate reaches more than 30%, the flexural strength of the specimen reaches more than 5.0 MPa at 28d curing age, which meets the requirements of flexural tensile strength of high-speed road and heavy traffic road (5.0 MPa).

(2) With the increasing amount of steel slag fine aggregate, the concrete splitting tensile strength increased from 1.95MPa, 2.31MPa and 2.94MPa to 2.73MPa, 2.81MPa and 4.04MPa, respectively, which indicates that steel slag fine aggregate has a positive effect on the development of concrete splitting tensile strength.

(3) C30 specimens with 30% steel slag doping have the shortest cracking time. As the steel slag based admixture increases, the later its cracking time under the same constraints, i.e., the worse the cracking resistance. Although C30 steel slag based concrete has high compressive strength, flexural strength as well as splitting tensile strength. However, due to its high modulus of elasticity and shrinkage, it is more prone to cracking as compared to other specimens.

Due to the limitation of time, manpower and material resources, the research on steel slag cement concrete in this paper still has a lot of shortcomings, for example, due to the test instrument, it fails to complete the abrasion resistance test of steel slag-based concrete, and it needs to be further researched on the abrasion resistance.

References

[1] Shankar, Ravi, A. U. , Palankar, Nitendra, Mithun, & B., M. . (2017). Investigations on alkali-activated slag/fly ash concrete with steel slag coarse aggregate for pavement structures. The international journal of pavement engineering.

[2] Farhan, N. A. , Sheikh, M. N. , & Hadi, M. N. S. . (2018). Engineering properties of ambient cured alkali-activated fly ash–slag concrete reinforced with different types of steel fiber. Journal of materials in civil engineering, 30(7), 04018142.1-04018142.12.

[3] Kumar, S. , Gupta, P. K. , & Iqbal, M. A. . (2024). Experimental and numerical study on self-compacting alkali-activated slag concrete-filled steel tubes. Journal of Constructional Steel Research, 214(Mar.), 1.1-1.18.

[4] Chen, C. , Chen, X. , Xu, W. , & Cheng, X. . (2021). Fracture behavior and crack mode of steel slag pervious concrete using acoustic emission technique. Structural Control and Health Monitoring(7).

[5] Nguyen, D. L. , Hang, N. T. T. , Hung, P. D. , & Ha, M. H. . (2020). Investigation on compressive characteristics of steel-slag concrete. Materials, 13(1928).

[6] Chai, C. , Cheng, Y. , Zhang, Y. , Zhu, B. , & Liu, H. . (2020). Mechanical properties of crumb rubber and basalt fiber composite modified porous asphalt concrete with steel slag as aggregate. Polymers(11).

[7] Xu, L. F. Z. Y. S. . (2021). Application of metallurgical steel slag in foamed concrete. Metalurgija, 60(1a2).

[8] Li, M. , Wang, Q. , Yang, J. , Guo, X. , & Zhou, W. . (2021). Strength and mechanism of carbonated solidified clay with steel slag curing agent. KSCE Journal of Civil Engineering, 25(3), 805-821.

[9] Sharba, A. A. . (2019). The efficiency of steel slag and recycled concrete aggregate on the strength properties of concrete. KSCE Journal of Civil Engineering, 23(5).

[10] Diotti, A. , Cominoli, L. , Adela Perèz Galvin, Sorlini, S. , & Plizzari, G. . (2021). Sustainable recycling of electric arc furnace steel slag as aggregate in concrete: effects on the environmental and technical performance. Sustainability, 13(2), 521.

[11] Kamath, K. . (2024). Evaluation of mechanical, ecological, economical, and thermal characteristics of geopolymer concrete containing processed slag sand. Sustainability, 16.

[12] Ren, C. . (2024). The impact of fly ash on the properties of cementitious materials based on slag-steel slag-gypsum solid waste. Materials, 17.

[13] Boquera, L. , Ramon Castro, J. , Fernandez, A. G. , Navarro, A. , Pisello, A. L. , & Cabeza, L. F. . (2022). Thermo-mechanical stability of concrete containing steel slag as aggregate after high temperature thermal cycles. Solar Energy.

[14] Liu, B. . (2020). Mechanical performance of steel slag concrete under biaxial compression. Materials, 13.

[15] Zeng, L. , Guo, P. , Wang, W. , Zhang, Y. , Wang, S. , & Peng, X. . (2020). Composite foamed alkali-activated concrete with slag and steel slag. Magazine of Concrete Research, 72(5/6), 262-270.

[16] Parron-Rubio María, Perez-García Francisca, Antonio, G. H. , & Rubio-Cintas María. (2018). Concrete properties comparison when substituting a 25% cement with slag from different provenances. Materials, 11(6), 1029.

[17] Li, L. , Ling, T. C. , & Pan, S. Y. . (2022). Environmental benefit assessment of steel slag utilization and carbonation: a systematic review. Science of The Total Environment, 806, 150280-.

[18] Zeynep, Y. I. , Umashankar, B. , & Monica, P. . (2023). Strength-gain characteristics and swelling response of steel slag and steel slag–fly ash mixtures. Journal of Materials in Civil Engineering.

[19] Loureiro, C. D. A. , Moura, C. F. N. , Rodrigues, M. , Martinho, F. C. G. , Silva, H. M. R. D. , & Oliveira, J. R. M. . (2022). Steel slag and recycled concrete aggregates: replacing quarries to supply sustainable materials for the asphalt paving industry. Sustainability, 14.

[20] Mo, L. , Zhang, F. , Deng, M. , Jin, F. , & Wang, A. . (2017). Accelerated carbonation and performance of concrete made with steel slag as binding materials and aggregates. Cement and Concrete Composites, 83, 138-145.

[21] Kim, S. , Kim, J. , Jeon, D. , Yang, J. , & Moon, J. . (2024). Enhanced mechanical property of steel slag through glycine-assisted hydration and carbonation curing. Cement and Concrete Composites, 149.

[22] Li, Y. , Yang, H. , Zhang, Y. , Zhao, Q. , Li, W. , & Zhu, Y. . (2022). Steel slag-red mud-based multi-solid waste pavement base material: preparation, properties and microstructure study. JOM(2), 74.

[23] Liu, J. , Yu, B. , & Wang, Q. . (2020). Application of steel slag in cement treated aggregate base course. Journal of Cleaner Production, 269, 121733.
[24] S., N. , & Brintha, G. S. . (2023). Utilization of slag powder and recycled concrete wastes in reactive powder concrete. Materiali in tehnologije.
[25] Zhijie Liu,Xibo Qi,Zhengkang Yu,Jia Ke,Xu Gao & Zhonghe Shui. (2024). Development and properties of cost-effective self-sensing Ultra-High Performance Fiber-Reinforced Concrete (UHPFRC) incorporating steel slags. Construction and Building Materials138502-138502.
[26] Wei Deng,Rui Xiong,Xinming Zhai,Kai Huang,Liding Li,Youjie Zong... & Fuyang Lu. (2024). Activation technology of steel slag for concrete exposed to plateau climate: a state-of-the-art review. Environmental science and pollution research international(44),1-18.